ijlpr 2022; doi 10.22376/ijpbs/lpr.2022.12.1.L1-10

International Journal of Life science and Pharma Research

ISSN 2250-0480

Research Article

Nanomaterial

Efficient photocatalytic degradation of organic dyes with Ag doped ZnO nanoparticles under UV light irradiation

M. Senthil Kumar[1], C. Arunagiri[2]*

[1]*Department of Physics, Srinivasan College of Arts and Science, (Affiliated to Bharathidasan University,Tiruchirapalli) Perambalur,Tamilnadu, India*

[2]*PG & Research Department of Physics, Periyar E.V.R College (Bharathidasan University, Tiruchirapalli), Tiruchirapalli, Tamilnadu,India*

Abstract: Semiconductor based photocatalyst for degradation of cationic and anionic dye pollutants under UV light was demonstrated for wastewater treatment. In the present work, un-doped and Ag (mol% = 0, 0.05, 0.075 and 0.1)-doped ZnO nanoparticles were synthesized by co-precipitation method. X-ray diffraction (XRD) pattern confirms that the samples are found to be of highly crystalline hexagonal wurtzite structure. Scanning electron microscopy (SEM) image reveals that the morphology of the doped ZnO nanoparticles are highly affected by the addition of silver (Ag). Fourier transform infra-red (FTIR) and energy-dispersive spectra (EDS) demonstrates the presence of Ag in the ZnO lattice. UV–Vis absorption spectra shows that the Ag-doped ZnO nanoparticles exhibit a red-shift with reduced bandgap energy compared with un-doped ZnO nanoparticles. Hence, our aim is to find the effect of Ag- doping in ZnO nanoparticles for the improvement of photocatalytic degradation. The photocatalytic activities of these Ag-doped nanoparticles were evaluated by measuring the rate of photo-degradation reaction of hazardous methylene blue (MB) and methyl orange (MO) dye under UV-light irradiation. Photocatalytic efficiency in the degradation of MB and MO dyes was compared with the efficiency of un-doped ZnO. The effects of various factors like solution pH, photocatalytic dosage and UV irradiation time with concentration of MB and MO on photocatalytic degradation were studied. It was found that cationic dyes shows better photo-degradation than the anionic dyes. The main objective of the present work was optimizing the various factor for better photocatalytic activity, complete mineralization and evaluating the photocatalytic-degradation mechanism.

Keywords:, Ag-Doping, Nanoparticles, Methylene Blue, Methyl Orange, Photocatalytic Degradation

***Corresponding Author**

C. Arunagiri , PG & Research Department of Physics, Periyar E.V.R College (Bharathidasan University, Tiruchirapalli), Tiruchirapalli, Tamilnadu,India

Received On 06 September 2021
Revised On 30 November 2021
Accepted On 08 December 2021
Published On 05 January 2022

Funding This research did not receive any specific grant from any funding agencies in the public, commercial or not for profit sectors.

Citation M. Senthil Kumar , C. Arunagiri , Efficient photocatalytic degradation of organic dyes with Ag doped ZnO nanoparticles under UV light irradiation.(2022).Int. J. Life Sci. Pharma Res.12(1), L1-10 http://dx.doi.org/10.22376/ijpbs/lpr.2022.12.1.L1-10

1. INTRODUCTION

Economically growing countries like India are facing environmental pollution due to industrial developments. In particular, industrial effluents discharged from cosmetics, textile, paper and paint industries contain high levels of organic contaminants including toxic chemicals and heavy metals[1]. Untreated industrial effluents release into water system has become one of the most serious water pollutions that severely affect the ecosystem and human health. Appropriate treatment is essential for effective destruction of effluents before they are released into the ecosystem[2]. There are several techniques available for the wastewater treatment such as activated carbon adsorption, chemical oxidation, coagulation, ion exchange, reverse osmosis, electrodialysis and advanced oxidation processes (AOP) have been found to be ineffective for the mineralization of toxic organic compounds[3-7]. Among them, photo-catalysis is an effective process that is used for heterogeneous photocatalytic degradation of organic effluents using a semiconductor as a photo-catalyst[8]. Many researchers are recently focused in conversion of organic dyes into harmless chemicals using photo-catalysts. ZnO is a versatile multifunctional wide band gap semiconductor like TiO_2 and it has numerous superior properties such as high electron transport, light sensitive, thermal and chemically stable, non-toxic and sustainable with hydrogen environment[9,10]. ZnO nanoparticles are effective photo-catalysts for degradation of toxic pollutants under UV irradiation. ZnO has better activity than TiO_2 for photocatalytic degradation of some organic dyes[11,12].The photocatalytic efficiency of ZnO nanoparticles mainly depends on the ability of electron–holes (e^-/h^+) pair formation under light illumination. However, the rapid recombination of photo-excited electron–holes (e^-/h^+), aggregation and low surface area of the bulk form are the main factors for the reduction of photocatalytic efficiency. Numerous methods, such as doping of metals and non-metals, combining with different semiconductors are used to overcome these drawbacks. The metal (Ag) doping of ZnO is most efficient way to improve its photocatalytic efficiency, because metal doping accelerates the charge carrier separation and change its physical and chemical properties[13-20]. ZnO has been prepared by a variety of techniques such as hydrothermal method[21], combustion[22], and sol-gel method[23]. Among these, co-precipitation[24] shows some advantages over the other methods. The present work explains the effect of various concentrations of Ag dopant on the structural and photocatalytic activity of ZnO nanoparticles. Furthermore, the samples were characterized by XRD, SEM, FTIR and UV-Vis spectrophotometer. To the best of our knowledge, this is the first report of application of Ag-doped ZnO nanoparticles for the degradation of cationic dye (methylene blue) and anionic dye (methyl orange) in water.

2. EXPERIMENTAL

2.1 MATERIALS AND METHODS

All the chemical used in the experiments are analytical grade and were used without further purification. Zinc nitrate hexahydrate [$Zn(NO_3)_2.6H_2O$], silver nitrate $Ag(NO_3)$, methylene blue (MB), methyl orange (MO) and sodium hydroxide [NaOH], were purchased from Alfa Aesar chemicals, India. Double distilled water (DDW) was used for all of the solutions.

2.2 Photo-catalyst Preparation

In a typical synthesis, 10 g of $Zn(NO_3)_2 \cdot 6H_2O$ was dissolved into 20 ml of DDW. In another container, 8 g of NaOH in 100 ml DDW. Then NaOH added to the zinc nitrate solution. Both these solutions were added dropwise under continuous magnetic stirring until pH adjusted into 11. Then the above solution was heated in in a vacuum oven at 150 °C for 1h. Afterwards, white color precipitates were separated by centrifugation and washed twice with DDW followed by ethanol and dried at 100 °C for 3h. The dried participate was calcined at 450 °C for 1h and finally un-doped ZnO nanoparticles formed. For synthesis of Ag doped ZnO nanoparticles containing various concentrations (mol% = 0.05, 0.075 and 0.1) of silver nitrate dissolved in water were added to the zinc nitrate solution with stirring. The co-precipitation method was selected based on available literature as described above[24]

2.3 Characterizations

The crystalline phases of un-doped and Ag-doped ZnO nanoparticles were determined by powder X-ray diffractometer (X'PERT PRO MPD) using CuKα radiation (λ = 0.15405 nm) operated at 40 kV voltage and 30 mA current with a scanning rate of 2° per min[21]. The particle size and morphological features of the samples were observed by scanning electron microscope (SEM-JEOL JS-6390) with energy dispersive X-ray spectrometer (EDX)[21]. Band gap energies of the samples were analysed from UV–visible spectra recorded using UV-Vis double-beam spectrophotometer (Systronics: AU-2707). Fourier Transform Infrared (FT-IR) spectra of prepared samples were recorded by using a FTIR Spectrometer (JASCO FTIR-410) in the range 400–4000 $cm^{-1}$with a resolution of 4 cm^{-1} at room temperature using KBr disc. Electrical characteristics (I-V) curve of the samples were carried out using a Keithley electrometer 2400 model

2.4 Evaluation of Photocatalytic activity

Photocatalytic activity of the un-doped and Ag-doped ZnO nanoparticles was evaluated for degradation of MB and MO dye solution under UV light irradiation. The photocatalytic procedure was conducted by adding 10 mg of photo-catalyst in 50 mL, 10 ppm of MB and MO dye solution. The reaction mixture was stirred for 30 min. under a dark to reach adsorption–desorption equilibrium. After that the dye solution was irradiated with an 8 W UV lamp was switched on. At different time intervals (0, 15, 30, 45, 60 and 75 min.) samples were taken out and centrifuged to separate the catalyst and then the supernatant was analysed in a UV-visible double beam spectrophotometer maximum wavelength (λmax) observed at ~664 and 464 nm to study the photocatalytic degradation. The photo-degradation efficiency (D%) of the MB and MO dye was calculated using the equation[25]

$$(D\%) = [C\text{-}C_0/C_0]\times 100$$

Where, C_0 and C are the initial and final degradation time of MB and MO (mg/L) dye solution used.

3. RESULT AND DISCUSSION

3.1 XRD Analysis

In order to investigate the crystal structure of un-doped ZnO and Ag doped ZnO nanoparticles were characterized by powder X-ray diffraction (PXRD) data. Fig. 1(a) depicts the PXRD patterns of un-doped ZnO and Ag doped ZnO nanoparticles with different concentrations of Ag, i.e. 0.05, 0.075 and 0.1%. The XRD pattern of all samples have strong diffraction peaks are assigned to (100), (002), (101), (102), (110), (103), (200), (112) and (201) planes of hexagonal wurtzite structure of ZnO in the Miller indices (JCPDS-36-1451) [26]. There is no extra peaks or other unidentified peaks corresponds to Ag or its oxide phases in the XRD pattern.

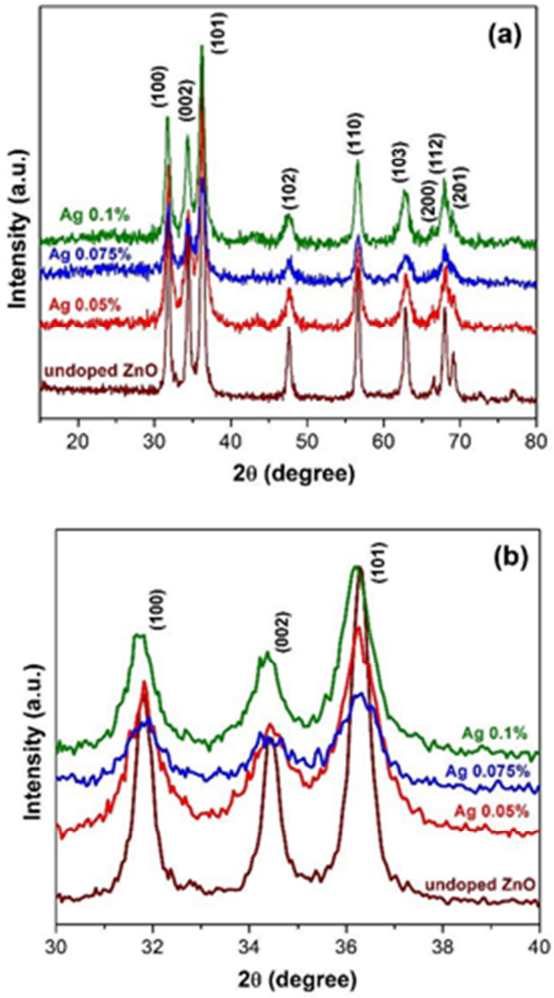

Fig. 1. (a) XRD patterns of un-doped and Ag-doped ZnO nanoparticles (b) expanded view of XRD patterns shift.

Table 1. Lattice parameters and crystallite size of undoped and Ag-doped ZnO nanoparticles.

Ag doping (mol%)	hkl	a[Å]	c[Å]	c/a	Average Crystallite Size (nm)
ZnO	100 002 101	3.2555	5.2184	1.6029	23
$Ag_{0.05}Zn_{0.95}O$	100 002 101	3.2562	5.2190	1.6028	20

	1				
$Ag_{0.075}Zn_{0.925}O$	100 002 101	3.2584	5.2210	1.6023	19
$Ag_{0.1}Zn_{0.9}O$	100 002 101	3.2586	5.2240	1.6031	18

Fig. 1(b) shows a magnification of the peak at 31.8 (100), 34.3 (002) and 36.3° (101) were a slight peak shift to lower angles observed in the 0.05, 0.075, and 0.1% Ag-doped ZnO nanoparticles. This result confirms that Ag impurity has been successfully incorporated into the ZnO lattice structure. The lattice constants and average crystallite size of major XRD peaks calculated for different samples are listed in Table 1. In our study, the effect of Ag doping on the average crystallite size (D) of was calculated for all samples by Debye–Scherrer's equation, and are found to be 23, 20, 19 and 18 nm, respectively[27].These results indicate that the D value in the Ag-doped ZnO nanoparticles decreased as the doping concentration increased. Furthermore, the increasing Ag content decreases the lattice parameters and average crystallite size values. Other studies have found the same results were reported by Pal *et al.*[28] in Co-doped ZnO nanoparticles, Saravanan *et al.*[29] in Ag-doped ZnO nanoparticles and Udom *et al.*[30] in Ag-doped ZnO nanowires.

3.2 SEM with EDX Analysis

The surface morphology and chemical composition of the prepared samples were investigated by SEM with EDX. SEM images of un-doped ZnO and Ag (0.05, 0.075 and 0.1 mol.%) doped ZnO nanoparticles are shown in Fig. 2(a-d). Fig. 2(a) shows the formation of irregular spherical morphology of the un-doped ZnO. From the Fig 2(b-d), it was precisely discovered that well prepared samples are in nanometer size and the surface morphology changes with the silver concentration. The variation of surface morphology with Ag dopant is due to the variation of number of nucleation sites[21]. The silver concentration reduces the particle size and it was confirmed from the XRD results. The obtained results are similar to the results reported by Pung et al[31].

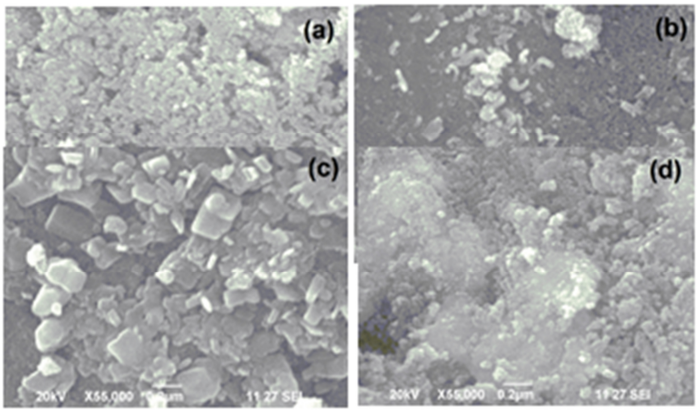

Fig. 2. SEM images of (a) undoped (b) 0.05, (c) 0.075 and (d) 0.1 mol.% Ag-doped ZnO nanoparticles.

The EDX spectra for un-doped ZnO and Ag (0.1%)-doped ZnO nanoparticles are shown in Fig. 3 (a, b). EDX spectrum of un-doped ZnO shows presence existence characteristic peaks of oxygen (O) and zinc (Zn) elements. The EDX pattern of Ag-doped nanoparticles also include elements such as existence of silver (Ag) together with Zn and O, indicating the successful doping of Ag in the ZnO matrix[31].

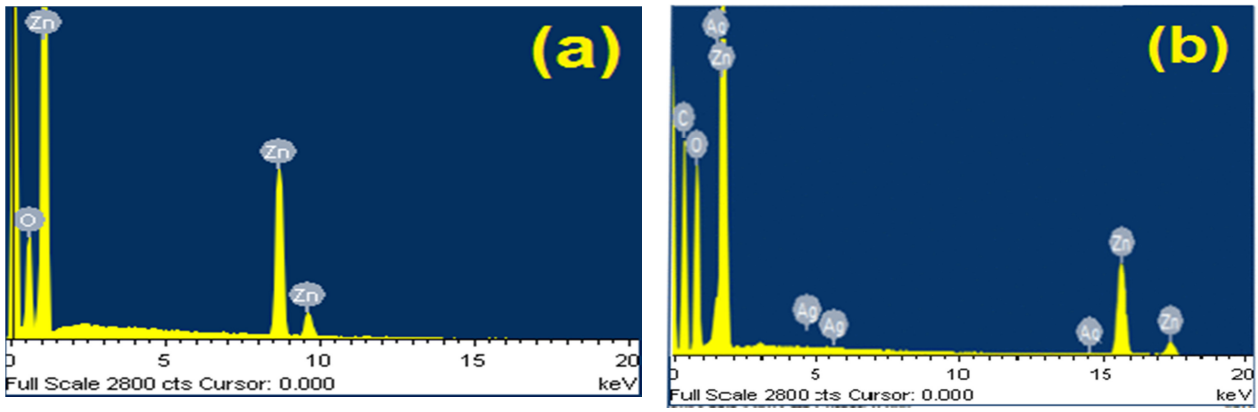

Fig. 3. EDX images of (a) un-doped and (b) 0.1 mol.% Ag-doped ZnO nanoparticles.

3.3 UV-Vis Analysis

In order to investigate the optical properties of un-doped ZnO and Ag (0.05, 0.075 and 0.1 mol.%) doped ZnO nanoparticles were investigated by UV-Vis. absorption spectroscopy. Fig. 4 (a-d) shows the UV-Vis absorption spectra of un-doped ZnO and Ag (0.05, 0.075 and 0.1 mol.%) doped ZnO nanoparticles. Un-doped ZnO has an absorption cut-off edge was observed around 370 nm. The adsorption of Ag-doped ZnO nanoparticles was shifted to the longer wavelength from ZnO with the increase of the molar ratio of Ag (0.05, 0.075 and 0.1 mol.%). After Ag-doping display an additional hump absorption in the visible region observed at 373, 375 and 377 nm. The calculated optical band gap energies were 3.35, 3.33, 3.30 and 3.28 eV for un-doped ZnO and Ag-doped ZnO nanoparticles, respectively. According to some previous reports similar result was observed by Hassan *et al.*[32].

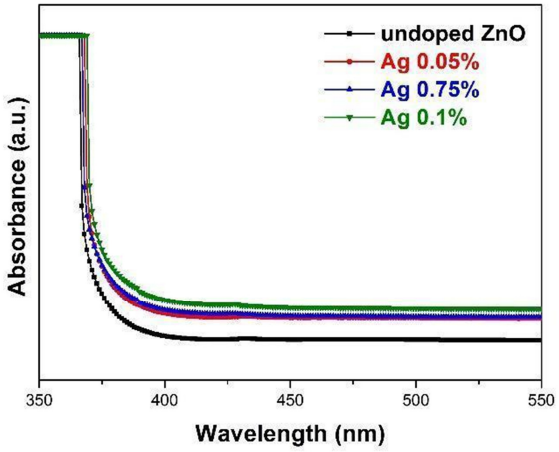

Fig. 4. UV-Vis absorbance spectra (a) un-doped (b) 0.05, (c) 0.075 and (d) 0.1 mol.% Ag-doped ZnO nanoparticles.

3.4 FT-IR Analysis

The FTIR spectra of un-doped ZnO and Ag (0.1%)-doped ZnO nanoparticles are presented in Fig. 5 (a, b). The absorption peaks present at 3441 and 1625 cm^{-1} which corresponds to the -OH stretching and bending vibration of the water molecule[33].

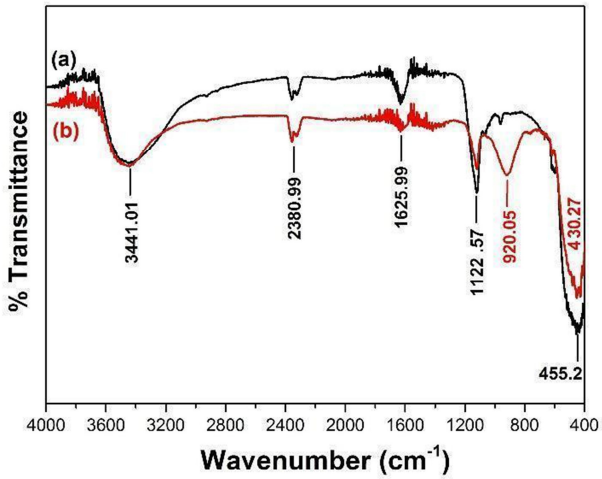

Fig. 5. FT-IR spectra of (a) un-doped and (b) 0.1 mol.% Ag-doped ZnO nanoparticles.

The band at 2380 cm^{-1} corresponds to symmetric and asymmetric C–H bond[34]. The observed FTIR spectrum exhibits several well-defined absorption bands at 1122 and 920 cm^{-1} and they are attributed to sulphate and C=C bonds, respectively[35]. The absorption peaks appears at 400 and 550 cm^{-1} were assigned to the metal–oxygen (M–O) stretching mode[36] and the absorbance peak noticed in the spectra around 455 and 430 cm^{-1} corresponds to the presence of Zn–O and Ag-O stretching bond, respectively.

3.5 I-V Characteristics

Electrical properties of un-doped ZnO and Ag (0.1%)-doped ZnO nanoparticles was measured by using the I-V characteristics and it is presented in Fig. 6 (a, b). From IV curves, electrical conductivity of un-doped ZnO and Ag (0.1%)-doped ZnO taken under varying temperatures from 30 to 130 °C.

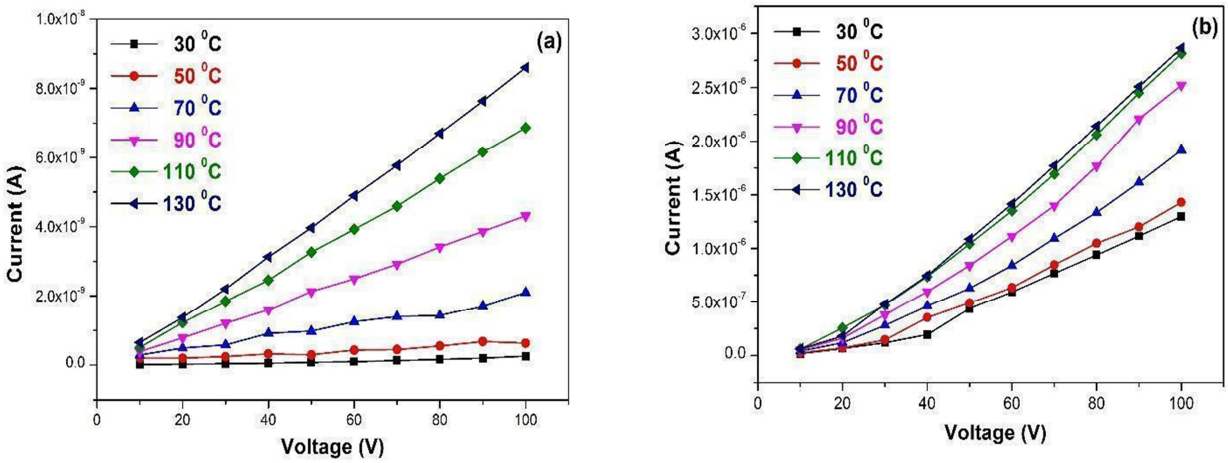

Fig. 6. I-V characteristics of (a) un-doped and (b) 0.1 mol.% Ag-doped ZnO nanoparticles.

This study reveals that (0.1%) Ag-doped ZnO nanoparticles shows better conductivity than the un-doped ZnO and it may due to the presence of more charge carrier's mobility[37].

3.6 Photocatalytic Activity

3.6.1 Optimized Factors to the Catalytic Activity

The photocatalytic degradation of un-doped ZnO and Ag-doped ZnO nanoparticles were selected for the evaluation of photocatalytic activity under UV-visible light. In order to study the effect of the UV light on the degradation of MB and MO dye. The dyes were prepared in various concentrations like acidic, neutral and alkaline medium. The photocatalytic activity was carried out and optimised for un-doped ZnO catalyst with MB and MO dye concentration of 10 ppm, catalyst concentration of 10 mg, pH = 6 and UV irradiation time up to 150 min.

3.6.2 Impact of UV irradiation on Degradation of MB and MO

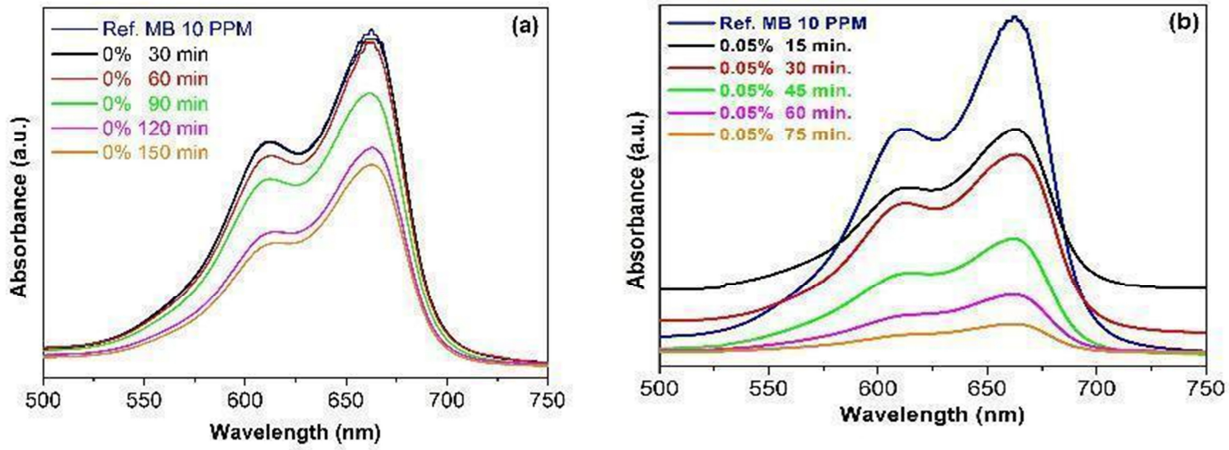

For the above mentioned conditions the photocatalytic degradation was carried out for Ag-doped ZnO nanoparticles. The Fig. 7(a-d) shows the comparative spectra of degradation of MB dye with un-doped ZnO and Ag (mol% = 0.05, 0.075, 0.1)-doped ZnO nanoparticles with respect to time. The high intensity absorption peaks was observed at 664 nm for MB dye. It was observed that the degradation of MB dye increases with increase of dopant concentration[24].

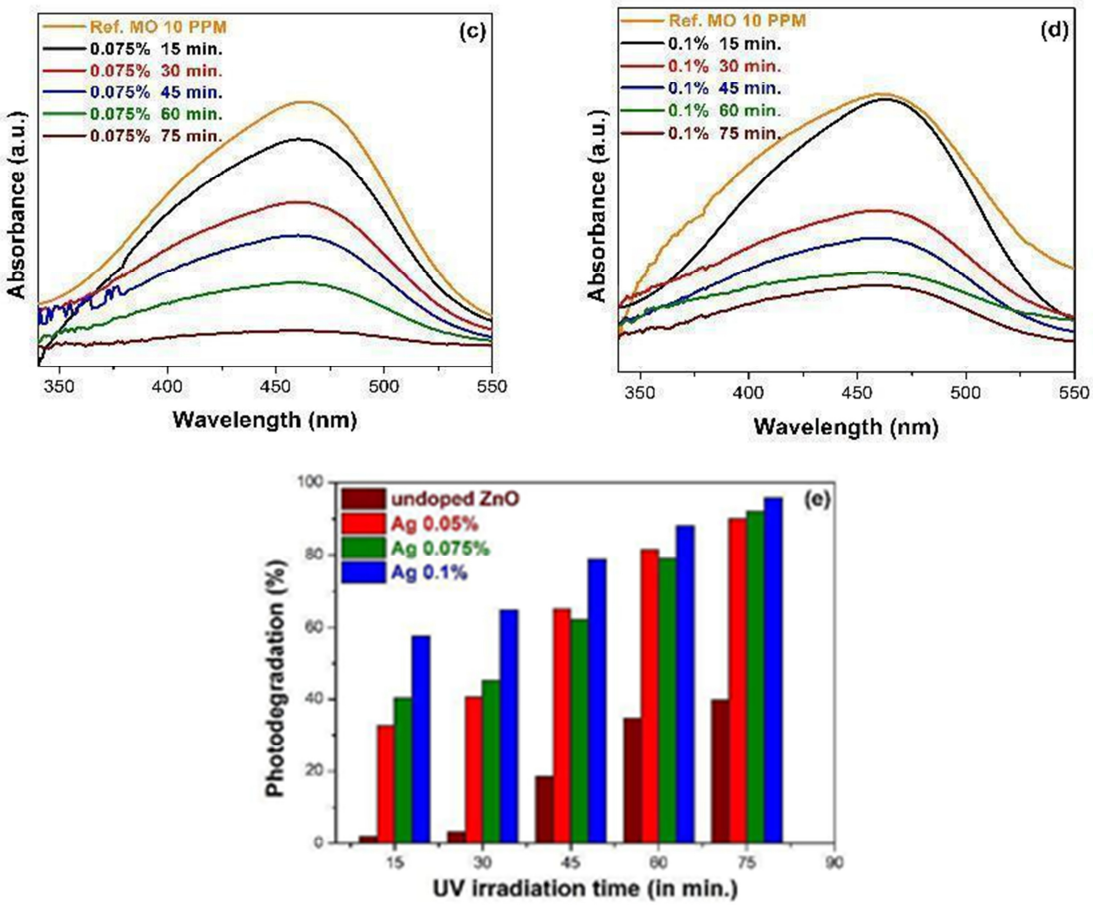

Fig. 7. MB dye degradation of (a) un-doped (b) 0.05, (c) 0.075, (d) 0.1 mol.% Ag-doped ZnO nanoparticles (MB dye:10 ppm, catalyst dose:10 mg, pH=6) and (e) effect of irradiation time of UV on MB photo-degradation.

The efficiency of un-doped and Ag-doped ZnO nanoparticles under UV light reaches 38, 90, 92 and 95% after 75 min light irradiation. Ag (0.1%)-doped ZnO nanoparticle shows the highest degradation efficiency of 95% under UV radiation for MB dye, while under similar conditions, a much lower efficiency (38%) was observed for un-doped ZnO nanoparticles under visible light radiation[24].

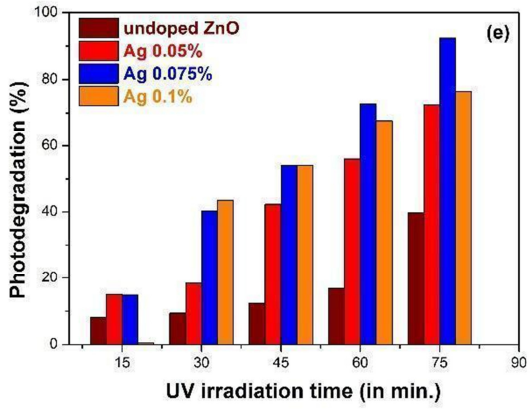

Fig. 8. MO dye degradation of (a) un-doped (b) 0.05, (c) 0.075, (d) 0.1 mol.% Ag-doped ZnO nanoparticles (MO dye:10 ppm,

catalyst dose:10 mg, pH=6) and (e) effect of irradiation time of UV on MO photo-degradation.The comparative spectra for degradation MO dye with un-doped ZnO and Ag (mol% = 0.05, 0.075, 0.1)-doped ZnO nanoparticles with respect to time was presented in Fig. 8(a-d). The high intensity absorption peaks of MO dye were observed at 464 nm. The effect of irradiation time of UV on MO dye degradation is shown in Fig. 8 (e). The degradation efficiency increases with increase of dopant concentration and the obtained values are 36, 72, 92 and 76%, respectively for un-doped, 0.05, 0.075 and 0.1 mol.% Ag-doped ZnO nanoparticles. It can be seen that maximum degradation (92%) of MO dye was achieved for Ag (0.075%)-doped ZnO nanoparticles in 75 min. It should be noted

that MB was degraded more faster than MO in the presence of the Ag-dopant. The possible photocatalytic degradation mechanism of MB and MO on Ag-doped ZnO nanoparticles under UV-visible light irradiation can be explained from the equation 1 to 6. During the catalytic process, photons can excite electrons in the valence band (VB) to be moved up to the conduct band (CB) and generate the same amount of electron-hole pair (e^- and h^+). The photo-excited electrons will be transferred from ZnO to Ag nanoparticles under the potential energy. The photocatalytic activity is effective thereby preventing the recombination between electrons and holes on the surface of ZnO. Afterwards, the electron on Ag nanoparticles can produce the $\cdot O_2^-$ superoxideradical, while the holes in the VB can react with H_2O_2 to produce $\cdot OH$ hydroxylradical[38]. These free radicals can degrade organic compounds to CO_2 and H_2O[31]

$$ZnO + h\gamma \longrightarrow ZnO(h^+_{VB} + e^-_{CB}) \quad (1)$$

$$ZnO\ (e^-_{CB}) + Ag \longrightarrow ZnO + Ag\ (e^-_{CB}) \quad (2)$$

$$Ag\ (e^-_{CB}) + O_2 \longrightarrow \cdot O_2^- + Ag \quad (3)$$

$$ZnO\ (h^+_{VB}) + H_2O \longrightarrow ZnO + H^+ + \cdot OH \quad (4)$$

$$(\cdot O_2^- + \cdot OH) + dye\ (MB\ or\ MO) \longrightarrow degradation\ products \quad (5)$$

$$(\cdot O_2^- + \cdot OH) + degradation\ products \longrightarrow CO_2 + H_2O \quad (6)$$

Products Till now, many studies have proven that electrons can transfer from Ag to the CB of ZnO. Then, they are scavenged by adsorbed O_2 molecules to yield superoxide radical anions ($\cdot O_2^-$) to degrade dye molecules[38]. Therefore, the photocatalytic activity will be enhanced.

4. CONCLUSION

In summary, various mol% of Ag-doped ZnO nanoparticles was synthesized using co-precipitation method. The structural, morphological, optical and electrical properties as well as the photocatalytic activity under UV irradiation of the resultant samples were characterized by XRD, SEM with EDX, UV–Vis FT-IR and IV analysis. Doping of Ag modified the morphology and average crystallite size of ZnO nanoparticles. In photocatalytic activity, Ag-doped ZnO nanoparticles enhances the degradation of MB dye under UV irradiation than the degradation of MO dye. The optimum reaction conditions for the degradation of MB and MO under UV-visible light irradiation of samples were pH= 6.0, catalyst dosage of 10 mg, and MB and MO concentration of 10 ppm. The possible mechanism of photocatalytic activity was studied and Ag enables the trapping of electrons in Ag-doped ZnO nanoparticles. Ag (0.1 mol%)-doped ZnO nanoparticles may be assumed as a promising photo-catalyst for the degradation of toxic organic effluents at room temperature.

5. AUTHOR CONTRIBUTION STATEMENT

Mr. Senthil Kumar, M conceptualized and gathered the data with regard to this work. Dr.Arunagiri, C analysed these data and supervised

6. CONFLICT OF INTEREST

Conflict of interest declared none.

7. REFERENCES

1. Pereira RA, Pereira MFR, Alves MM, Pereira L. Carbon based materials as novel redox mediators for dye wastewater biodegradation. Appl Catal B. 2014;144:713-20. doi:10.1016/j.apcatb.2013.07.009.
2. Umar A, Akhtar MS, Al-Hajry A, Al-Assiri MS, Dar GN, Saif Islam M. Enhanced photocatalytic degradation of harmful dye and phenyl hydrazine chemical sensing using ZnO nanourchins. Chem Eng J. 2015;262:588-96. doi:10.1016/j.cej.2014.09.111.
3. Gao B, Liu B, Chen T, Yue Qinyan. Effect of aging period on the characteristics and coagulation behavior of polyferric chloride and polyferric chloride–polyamine composite coagulant for synthetic dying wastewater treatment. J Hazard Mater. 2011; 187(1-3): 413-20. doi:10.1016/j.jhazmat.2011.01.044, PMID 21295910.
4. Szyguła A, Guibal E, AriñoPalacín MA, Ruiz M, Sastre AM. Removal of an anionic dye (Acid Blue 92) by coagulation–flocculation using chitosan. J Environ

Manage. 2009;90(10):2979-86. doi:10.1016/j.jenvman.2009.04.002, PMID 19467769.
5. Kim T-H, Park Chulhwan, Kim Sangyong. Water recycling from desalination and purification process of reactive dye manufacturing industry by combined membrane filtration. J Clean Prod. 2005;13(8):779-86. doi: 10.1016/j.jclepro.2004.02.044.
6. Gupta VK, Pathania D, Agarwal S, Singh P. Adsorptional photocatalytic degradation of methylene blue onto pectin–CuS nanocomposite under Solar Light. J Hazard Mater. 2012;243:179-86. doi: 10.1016/j.jhazmat.2012.10.018, PMID 23122730.
7. Körbahti BK, Artut K, Geçgel C, Özer A. Electrochemical decolorization of textile dyes and removal of metal ions from textile dye and metal ion binary mixtures. Chem Eng J. 2011;173(3):677-88. doi: 10.1016/j.cej.2011.02.018.
8. Umar A, Akhtar MS, Al-Hajry A, Al-Assiri MS, Almehbad NY. Hydrothermally grown ZnO nanoflowers for environmental remediation and clean energy applications. Mater Res Bull. 2012;47(9):2407-14. doi: 10.1016/j.materresbull.2012.05.028.
9. Jagadhesan S, Senthilkumar N, Senthilnathan V, Senthil TS. Sb doped ZnO nanostructures prepared via co precipitation approach for the enhancement of MB dye degradation. Mater Res Express. 2018;5(2):025040. doi: 10.1088/2053-1591/aaaf80.
10. Tu VA, Tuan VA. A facile and fast solution chemistry synthesis of porous ZnO nanoparticles for high efficiency photodegradation of tartrazine. Viet J Chem. 2018;56(2):214-9. doi: 10.1002/vjch.201800016.
11. Shafaei A, Nikazar MM, Arami M. Photocatalytic degradation of terephthalic acid using titania and zinc oxide photocatalysts: comparative study. Desalination. 2010;252(1-3):8-16. doi: 10.1016/j.desal.2009.11.008.
12. Xie J, Li Y, Zhao W, Bian L, Wei Y. Simple fabrication and photocatalytic activity of ZnO particles with different morphologies. Powder Technology. 2011;207(1-3):140-4. doi: 10.1016/j.powtec.2010.10.019.
13. Subash B, Krishnakumar B, Swaminathan M, Shanthi M. Synthesis and characterization of cerium–silver co-doped zinc oxide as a novel sunlight-driven photocatalyst for effective degradation of Reactive Red 120 dye. Mater Sci Semicond Process. 2013;16(4):1070-8. doi: 10.1016/j.mssp.2013.04.001.
14. Araújo ES, da Costa BP, Oliveira RAP, Libardi J, Faia PM, de Oliveira HP. TiO2/ZnO hierarchical hetero nanostructures: synthesis, characterization and application as photocatalysts. J Environ Chem Eng. 2016;4(3):2820-9. doi: 10.1016/j.jece.2016.05.021.
15. Neelakanta Reddy I, Venkata Reddy Ch, Shim J, Akkinepally B, Cho M, Yoo K, Kim D. Excellent visible-light driven photocatalyst of (Al, Ni) co-doped ZnO structures for organic dye degradation. Cat Today. 2018;340:277-85.
16. Bera A, Basak D. Photoluminescence and photoconductivity of ZnS-coated ZnO nanowires. ACS Appl Mater Interfaces. 2010;2(2):408-12. doi: 10.1021/am900686c, PMID 20356186.
17. Li BX, Wang YF. Facile synthesis and photocatalytic activity of ZnO–CuO nanocomposite. Superlattices and Microstructures. 2010;47(5):615-23. doi: 10.1016/j.spmi.2010.02.005.
18. Lei YZ, Zhao GH, Liu MC, Zhang ZN, Tong XL, Cao TC. Fabrication, characterization, and photoelectrocatalytic application of ZnO nanorods grafted on vertically aligned TiO2 nanotubes. J Phys Chem C. 2009;113(44):19067-76. doi: 10.1021/jp9071179.
19. Zhang ZY, Shao CL, Li XH, Wang CH, Zhang MY, Liu YC. Electrospun nanofibers of p-type NiO/n-type ZnO heterojunctions with enhanced photocatalytic activity. ACS Appl Mater Interfaces. 2010;2(10):2915-23. doi: 10.1021/am100618h, PMID 20936796.
20. Wang Q, Geng BY, Wang SZ. ZnO/Au hybrid nanoarchitectures: wet-chemical synthesis and structurally enhanced photocatalytic performance. Environ Sci Technol. 2009;43(23):8968-73. doi: 10.1021/es902568h, PMID 19943674.
21. Sriharan N, Muthukumarasamy N, Thambidurai M, Senthil TS. Importance of ZnO nanorods prepared from hydrothermal method for various dyes degradation. J Optoelectron Adv Mater. 2017;19(9-10):634-40.
22. Tarwal NL, Jadhav PR, Vanalakar SA, Kalagi SS, Pawar RC, Shaikh JS, Mali SS, Dalavi DS, Shinde PS, Patil PS. Photoluminescence of zinc oxide nanopowders synthesized by a combustion method. Powder Technol. 2011;208(1):185-8. doi: 10.1016/j.powtec.2010.12.017.
23. Alireza Samadi Tabrizi. Investigating various factors to increase the strength of alumina nano-fibers using sol-gel method. Int J Life Sci Pharma Res. 2016;6(4):1-11.
24. Jagadhesan S, Senthilnathan V, Senthil TS. Studies on Diamond like Sn doped ZnO nanostructures prepared via co-precipitation approach for improving photo-catalytic application. J Optoelectron Adv Mater. 2018;20:188-95.
25. Davoud Balarak, Marzieh Baniasadi, Kethineni Chandrika. Investigating the efficiency of zirconium oxide nanoparticles in removal ofciprofoxacin from aqueous environments. Int J Life Sci Pharma Res., 2020;10(1):17-22.
26. Ashkarran AA, Irajizad A, Mahdavi SM, Ahadian MM. ZnO nanoparticles prepared by electrical arc discharge method in water. Mater Chem Phys. 2009;118(1):6-8. doi: 10.1016/j.matchemphys.2009.07.002.
27. Nasir M, Bagwasi S, Jiao Y, Chen F, Tian B, Zhang J. Characterization and activity of the Ce and N co-doped TiO2 prepared through hydrothermal method. Chem Eng J. 2014;236:388-97. doi: 10.1016/j.cej.2013.09.095.
28. Pal B, Giri PK. Defect mediated magnetic interaction and high Tc ferromagnetism in Co doped ZnO nanoparticles. J Nanosci Nanotechnol. 2011;11(10):9167-74. doi: 10.1166/jnn.2011.4293, PMID 22400318.
29. Saravanan S, Silambarasan M, Soga T. Structural, morphological and optical studies of Ag-doped ZnO nanoparticles synthesized by simple solution combustion method. Jpn J Appl Phys. 2014;53(11S). doi: 10.7567/JJAP.53.11RF01.

30. Udom I, Zhang Y, Ram MK, Stefanakos EK, Hepp AF, Elzein R, Schlaf R, Goswami DY. A simple photolytic reactor employing Ag-doped ZnO nanowires for water purification. Thin Solid Films. 2014;564:258-63. doi: 10.1016/j.tsf.2014.05.057.
31. Pung SY, Lee WP, Aziz A. Kinetic study of organic dye degradation using ZnO particles with different morphologies as a photocatalyst. Int J Inorg Chem. 2012;2012:1-9:Article ID 608183. doi: 10.1155/2012/608183.
32. Mehedi Hassan MM, Khan W, Azam A, Naqvi AH. Influence of Cr incorporation on structural, dielectric and optical properties of ZnO nanoparticles. J Ind Eng Chem. 2015;21:283-91. doi: 10.1016/j.jiec.2014.01.047.
33. Jiménez-González AE, Soto Urueta JAS, Suárez-Parra R. Optical and electrical characteristics of aluminum-doped ZnO thin films prepared by sol–gel technique. J Cryst Growth. 1998;192(3-4):430-8. doi: 10.1016/S0022-0248(98)00422-9.
34. Ramimoghadam D, Hussein MZB, Taufiq-Yap YH. Synthesis and characterization of ZnO nanostructures using palm olein as biotemplate. Chem Cent J. 2013;7(1):71. doi: 10.1186/1752-153X-7-71, PMID 23601826.
35. Saoud K, Alsoubaihi R, Bensalah N, Bora T, Bertino M, Dutta J. Synthesis of supported silver nano-spheres on zinc oxide nanorods for visible light photocatalytic applications. Mater Res Bull. 2015;63:134-40. doi: 10.1016/j.materresbull.2014.12.001.
36. Srivastava M, Ojha AK, Chaubey S, Sharma PK, Pandey AC. Influence of calcinations temperature on physical properties of the nanocomposites containing spinel and CuO phases. J Alloys Compd. 2010;494(1-2):275-84. doi: 10.1016/j.jallcom.2010.01.008.
37. Abed S, Bougharraf H, Bouchouit K, Sofiani Z, Derkowska-Zielinska B, Aida MS, Sahraoui B. Influence of Bi doping on the electrical and optical properties of ZnO thin films. Superlattices Microstruct. 2015;85:370-8. doi: 10.1016/j.spmi.2015.06.008.
38. Mittal M, Sharma M, Pandey OP. UV–visible light induced photocatalytic studies of Cu doped ZnO nanoparticles prepared by co-precipitation method. Sol Energy. 2014;110:386-97. doi: 10.1016/j.solener.2014.09.026.